Inorganic Chemistry

Article

pubs.acs.org/IC

# Solvent-Induced Syntheses, Crystal Structures, Magnetic Properties, and Single-Crystal-to-Single-Crystal Transformation of Azido-Cu(II) Coordination Polymers with 2-Naphthoic Acid as Co-ligand

Xiangyu Liu,[†,‡] Peipei Cen,[‡] Hui Li,[§] Hongshan Ke,[†] Sheng Zhang,[†] Qing Wei,[†] Gang Xie,[†] Sanping Chen,*[,†] and Shengli Gao[†]

[†]Key Laboratory of Synthetic and Natural Functional Molecule Chemistry of Ministry of Education, College of Chemistry and Materials Science, Northwest University, Xi'an 710069, China

[‡]School of Chemistry and Chemical Engineering, Ningxia University, Yinchuan 750021, China

[§]College of Chemistry and Chemical Engineering, North University for Nationalities, Yinchuan 750021, China

Supporting Information

**ABSTRACT:** Based on the solvent-induced effect, three new azido-copper coordination polymers—[Cu(2-na)($N_3$)] (**1**), [Cu(2-na)($N_3$)] (**2**), and [Cu(2-na)($N_3$)($C_2H_5OH$)] (**3**) (where 2-na = 2-naphthoic acid)—have been successfully prepared. Structure analysis shows that the Cu(II) cations in compounds **1**−**3** present tetra-, penta-, and hexa-coordination geometries, respectively. Compound **1** is a well-isolated one-dimensional (1D) chain with the EO-azido group, while **2** is an isomer of **1** and exhibits a two-dimensional (2D) layer involving the EE-azido group. Thermodynamically, density functional theory (DFT) calculation reveals that **2** occupies the stable state and **1** locates in the metastable state. Compound **3** consists of a 1D chain with triple bridging mode, which is derived from **1**, and undergoes a single-crystal-to-single-crystal transformation by soaking in ethanol solvent; the powdery product of **1**, namely **1b**, could be yielded after the dealcoholization of compound **3**. Magnetic measurements indicate that compounds **1**−**3** perform strong intrachain ferromagnetic interactions, experiencing long-range magnetic ordering and slow magnetic relaxation. Compound **1** features the metamagnetic behavior with a transition temperature of 15 K, while **2** and **3** display spin glass behavior with the phase transition temperatures of 15 and 12 K, respectively. Magneto-structure relationships are investigated as well.

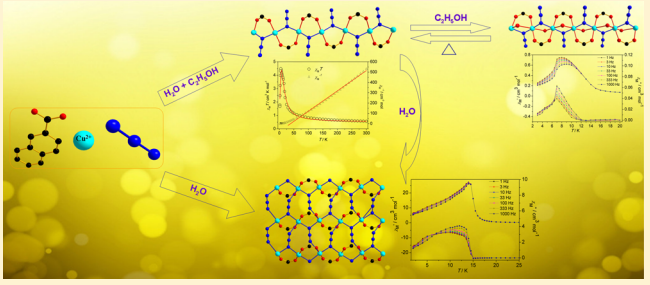


## INTRODUCTION

Structural design and magnetic properties of coordination polymers (CPs) are presently of considerable interest.[1] In particular, the advancements of low-dimensional magnetic CPs, for instance, single-molecule magnets (SMMs),[2] single-chain magnets (SCMs),[3] and others displaying low-dimensional magnetic characteristics such as metamagnetism.[4] As observed, single-chain compounds exhibit slow magnetic relaxation resulting from significant uniaxial anisotropy, as well as large intrachain and weak interchain magnetic interactions. Coordination chemistry acts as a potent tool for approaching chainlike compounds in which short bridging ligands ($CN^-$, $SCN^-$, $N^{3-}$, etc.) are often employed to bridge paramagnetic metal ions and then to transmit magnetic exchange.[5] As a basic spin carrier, the Cu(II) cation has received attention as a desired candidate for exploiting advanced molecule-based magnetic materials, further for comprehending the basal principle of magnetic interaction and the relationship between structure and magnetism in molecular system.[6] The versatile bridging ligand, $N_3^-$, is able to bridge metal centers in end-on (EO) mode, end-to-end (EE) mode, or other modes, leading to a number of low-dimensional (one-dimensional (1D)[7] or two-dimensional (2D)[8]) materials (see Scheme 1), with abundant structural variety and a series of diverse magnetic behaviors.[9] It is well-determined that the end-

**Scheme 1. Coordination Modes of Bridging Azido**

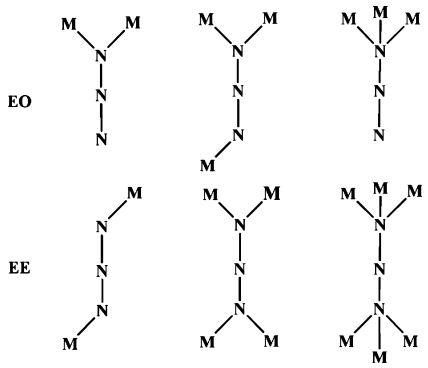


**Received:** May 11, 2014
**Published:** July 11, 2014

   dx.doi.org/10.1021/ic5010769 | *Inorg. Chem.* 2014, 53, 8088−8097

**Scheme 2. Syntheses of Compounds**

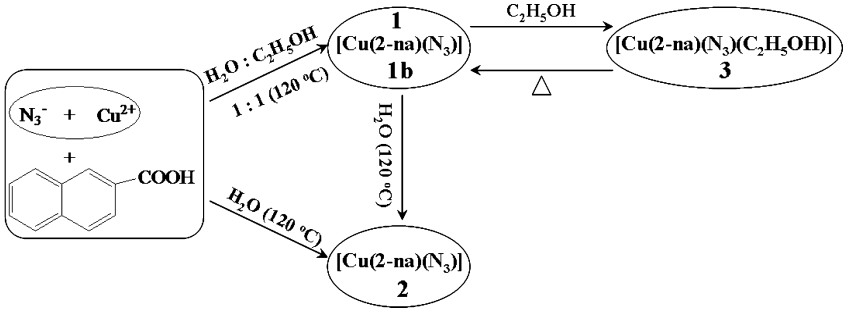


to-end mode generally transmits antiferromagnetic (AF) coupling while the end-on mode encourages ferromagnetic coupling, although the interaction between Cu(II) cations linked by EO modes could be antiferromagnetism in the presence of co-ligands. Meanwhile, geometrical parameters such as Cu−N−Cu angle and Cu−Cu distance have also important influence on the magnetic exchanges.[10] Obviously, it is effective strategy to introduce the co-ligands tuning the structures and, thus, the magnetic behaviors of azido-copper systems.[11] The carboxylate group becomes a well-known co-ligand that can bridge Cu(II) cations to generate multitudinous compounds and adopt different bridging conformations (*syn*−*syn*, *anti*−*anti*, etc.) to transmit diverse magnetic properties.[12] In the present work, we research the use of 2-naphthoic acid (2-na) with rigid structure as co-ligands into azido-Cu(II) systems.

Beyond that, tuning the structures and properties of CPs still remains the significant challenge that is derived from some experimental conditions such as solvent, pH, and temperature exert important impacts on the structures of compounds.[13] Of particular concern is that the solvents usually affect the coordination behaviors of metal cations, which may determine the connection and dimension of the structural framework. Many reports concerning structure and magnetism fine-tuned by solvent have been performed,[14] in which the single-crystal-to-single-crystal (SCSC) transformation induced by solvent have attracted great interest, because of their intrinsic structural features.[15] The SCSC transformations contain mainly two types of structural changes: (i) interposition/deletion of guest molecules[16] and (ii) alteration in the coordinated environment of metal cations.[17] The latter type is rare because it involves the rupture of chemical bonds and generation of new products. All in all, the special phenomenon of SCSC is often impeded, as the loss of single crystal integrity during the transformation is frequent. To date, only a handful of cases have been reported, much less in metal azido systems.

Fortunately, we successfully prepared three azido Cu(II) compounds based on 2-naphthoic acid as the co-ligand. Noteworthily, two isomeric compounds, [Cu(2-na)($N_3$)] (**1**) and [Cu(2-na)($N_3$)] (**2**), are synthesized in specific solvents under hydro(solvo)thermal conditions, forming different structures of 1D chain and 2D layer, respectively. The thermodynamical stabilities of **1** and **2** are evaluated by DFT calculation. In particular, **1** undergoes a SCSC transformation to yield compound **3** with the formula of [Cu(2-na)($N_3$)-($C_2H_5OH$)], which structurally exhibits a triple-bridged 1D chain including the ethanol solvent molecule bridges adjacent Cu(II) cations. As we expected, the dealcoholization of **3** produces the powder phase of **1**. For three compounds, the structural formations are effected by using different solvent, resulting in diverse magnetic properties which have been systematically characterized. The correlations of structure and magnetism are also discussed.

## EXPERIMENTAL SECTION

**Physical Measurements.** The FT-IR spectra were recorded in the range of 400−4000 $cm^{-1}$ using KBr pellets on an EQUINOX55 FT/IR spectrophotometer. Elemental analysis (C, H, N) was implemented on a Perkin−Elmer 2400 CHN elemental analyzer. The phase purity of the bulk or polycrystalline samples were confirmed by powder X-ray diffraction (PXRD) measurements executed on a Rigaku RU200 diffractometer at 60 kV, 300 mA, and Cu K$\alpha$ radiation ($\lambda$ = 1.5406 Å), with a scan speed of 5° $min^{-1}$ and a step size of 0.02° in 2$\theta$. Magnetic measurements were accomplished on polycrystalline samples (10.17 mg for **1**, 14.21 mg for **2**, 11.69 mg for **3**) using a Quantum Design MPMS-XL7 SQUID magnetometer at temperatures between 1.8 and 300 K for direct current (dc) applied fields with the applied field of 1 kOe (restrained in eicosane to prevent torqueing at high fields). Alternating current (ac) susceptibility experiments for compounds were performed using an oscillating ac field of 3.5 Oe with the frequencies of 1, 3, 10, 33, 100, 333, and 1000 Hz. Magnetization versus field ($M/H$) variations were measured between 7 and −7 kOe at different temperatures. The measured susceptibilities were corrected for the diamagnetism of the constituent atoms (Pascal's tables).

**General Procedures and Materials.** All reagents and solvents were purchased and used without further purification.

*CAUTION!* Azido compounds are that of potentially explosives. Only a small amount of the title compounds should be prepared and handled with care.

**Synthesis of [Cu(2-na)($N_3$)]$_n$ (1).** A mixed aqueous ethanol (8 mL, 1:1) of $Cu(NO_3)_2{\cdot}3H_2O$ (0.072 g, 0.3 mmol), 2-na (0.019 g, 0.1 mmol) and $NaN_3$ (0.013 g, 0.2 mmol) was heated in a Teflon-lined bomb (15 mL) at 120 °C for 3 days, slowly cooled to room temperature (5 °C $h^{-1}$) (seee Scheme 2). Green flaky crystals of compound **1** were collected (yield 62%, based on Cu). Anal. Calcd for $CuC_{11}H_7N_3O_2$ (276.74): C, 47.70; H, 2.53; N, 15.18%. Found: C, 47.67; H, 2.51; N, 15.13%. Main IR (KBr, $cm^{-1}$): 2100 (s), 1593 (m), 1541 (s), 1410 (s), 1274 (w), 1112 (m), 911 (w), 788 (m), 614 (m).

**Synthesis of [Cu(2-na)($N_3$)]$_n$ (2).** The compound **2** was obtained from the following two ways:

(i) The method described above for **1**, but with the mixed aqueous ethanol with aqueous solution (Scheme 2). Green flaky crystals of compound **2** were collected. (yield 83%, based on Cu). Anal. Calcd for $CuC_{11}H_7N_3O_2$ (276.74): C, 47.70; H, 2.53; N, 15.18%. Found: C, 47.63; H, 2.46; N, 15.10%. Main IR (KBr, $cm^{-1}$): 2083 (s), 1632 (s), 1527 (s), 1472 (s), 1415 (s), 1295 (m), 1111 (m), 866 (w), 780 (m), 604 (m).

(ii) The aqueous solution (8 mL) of compound **1** was heated in a Teflon-lined bomb (15 mL) at 120 °C for 3 days, slowly cooled to room temperature (5 °C $h^{-1}$), the crystals of compound **2** were also obtained (Scheme 2).

**Synthesis of [Cu(2-na)($N_3$)($C_2H_5OH$)]$_n$ (3).** Single crystals of compound **1** (1.0 mmol, 0.277 g) were soaked into ethanol solution (30 mL), which yielded green stripe crystals of **3** within 7 days at room temperature (Scheme 2). Anal. Calcd for $CuC_{13}H_{13}N_3O_3$ (322.80): C,


dx.doi.org/10.1021/ic5010769 | Inorg. Chem. 2014, 53, 8088−8097

48.33; H, 4.03; N, 13.01%. Found: C, 48.28; H, 3.98; N, 12.06%. Main IR (KBr, $cm^{-1}$): 3418 (s), 2974 (m), 2088 (s), 1620 (m), 1582 (w), 1546 (s), 1503 (w), 1469 (m), 1413 (s), 1307 (m), 1079 (m), 1040 (m), 872 (m), 787 (s), 604 (m).

**Synthesis of $[Cu(2\text{-na})(N_3)]_n$ (1b).** **3** was put into a drying tube furnace and heating was maintained at 140 °C for half an hour under $N_2$ atmosphere (Scheme 2). Green powders of **1b** were obtained. Anal. Calcd for $CuC_{11}H_7N_3O_2$ (276.74): C, 47.70; H, 2.53; N, 15.18%. Found: C, 47.64; H, 2.50; N, 15.15%. Main IR (KBr, $cm^{-1}$): 2090 (s), 1586 (m), 1543 (s), 1418 (s), 1270 (w), 1107 (m), 913 (w), 788 (m), 612 (m).

**Crystallographic Data Collection and Refinement.** The single-crystal X-ray experiment was performed on a Rigaku SCX mini CCD diffractometer equipped with graphite-monochromatized Mo K$\alpha$ radiation ($\lambda$ = 0.71073 Å) using $\omega$ and $\varphi$ scan mode. The data integration and reduction were processed with SAINT software. Absorption correction based on multiscan was performed using the SADABS program.[18a] The structures were solved by the direct method using SHELXTL and refined by means of full-matrix least-squares procedures on $F^2$ with SHELXL-97 program.[18b] All nonhydrogen atoms were refined anisotropically. Other details of crystal data, data collection parameters, and refinement statistics are given in Table 1.The selected bond lengths and angles are listed in Table S1 in the Supporting Information.

**Table 1. Crystal Data and Structure Refinement Details for Compounds 1−3**

| | 1 | 2 | 3 |
|---|---|---|---|
| empirical formula | $CuC_{11}H_7N_3O_2$ | $CuC_{11}H_7N_3O_2$ | $CuC_{13}H_{13}N_3O_3$ |
| formula weight | 276.74 | 276.74 | 322.80 |
| crystal system | monoclinic | orthorhombic | monoclinic |
| space group | $P2(1)/c$ | $P2(1)2(1)2(1)$ | $P2(1)$ |
| $a$ (Å) | 9.249(2) | 5.0621(17) | 7.6816(14) |
| $b$ (Å) | 6.7980(16) | 6.579(2) | 6.3608(11) |
| $c$ (Å) | 16.707(4) | 31.087(10) | 14.582(3) |
| $\alpha$ (deg) | 90 | 90 | 90 |
| $\beta$ (deg) | 100.275(5) | 90 | 102.898(3) |
| $\gamma$ (deg) | 90 | 90 | 90 |
| $V$ ($Å^3$) | 1033.6(4) | 1035.3(6) | 694.5(2) |
| $Z$ | 4 | 4 | 2 |
| $\mu$ ($mm^{-1}$) | 2.103 | 2.100 | 1.582 |
| unique reflections | 1812 | 2097 | 1951 |
| observed reflections | 4926 | 5629 | 3463 |
| $R_{int}$ | 0.0887 | 0.1170 | 0.0606 |
| Final $R$ indices [$I > 2\sigma(I)$] | $R_1$ = 0.0563, $wR_2$ = 0.0725 | $R_1$ = 0.0662, $wR_2$ = 0.1392 | $R_1$ = 0.0562, $wR_2$ = 0.1006 |
| $R$ indices (all data) | $R_1$ = 0.1037, $wR_2$ = 0.0837 | $R_1$ = 0.1541, $wR_2$ = 0.1977 | $R_1$ = 0.0904, $wR_2$ = 0.1123 |

## RESULTS AND DISCUSSION

**Crystal Structure of 1.** X-ray determination reveals that compound **1** is composed of 1D azido-Cu chains. Cu(II) cations located at the inversion center adopts a square-planar geometry occupied by two azide nitrogen atoms (N1 and N1A) and two carboxylate oxygen atoms (O1 and O1A). The Cu−N and Cu−O distances are 1.974, 1.971, 1.918, and 1.933 Å, respectively (Figure 1a). Adjacent Cu(II) cations are bridged by an azido group with $\mu$-1,1-(EO) mode and a carboxylate group with *syn*−*syn* mode, yielding a formally EO-azido/carboxylate hybrid-bridged 1D chain (Figure 1b). The distance of adjacent Cu(II) cations is 3.433 Å in the 1D chain, while the Cu1−N1−Cu1A bond angle is 120.9°, which are in the normal range of EO bridging mode.[19] The 1D chains are connected by hydrogen bonding, forming the three-dimensional (3D) network in the lattice (see Figure S1 in the Supporting Information). The closest distance of interchain Cu(II) cations is 8.155 Å.

**Crystal Structure of 2.** In **2**, the 2D layer can be considered as the integration of 1D chains in **1**. Unlike **1**, the Cu(II) cations in **2** exhibit a penta-coordinated environment occupied by three azide N atoms and two carboxylate O atoms [Cu1−N1 = 1.981 Å, Cu1−N1A = 2.001 Å, Cu1−O1 = 1.917 Å, Cu1−O2 = 1.923 Å, and Cu1−N3 = 2.608 Å] (Figure 2a), producing a slightly distorted tetragonal pyramidal geometry. Adjacent two Cu(II) cations are bridged by a carboxylate group with *syn*−*syn* mode and the azido group with $\mu$-1,1,3 mode, giving a formally EO-azido/carboxylate hybrid-bridged 1D copper chain like **1** (Figure 2b), then the 1D copper chains are combined by $\mu$-(1,1,3)-$N_3$ to form a 2D layer (Figure 2c). The noncoplanar case occurs between the carboxylate group and naphthalene ring with the angle of 16°. The Cu−N−Cu and Cu−N3−N2 bond angles are 111.7° and 115.1°, respectively. The distances of three Cu(II) cations linked by one azido group are 3.295, 5.062, and 5.893 Å, respectively. Each azido links three Cu(II) cations when each Cu(II) cation coordinates with three azido groups in **2**. A simplified graphic of the 2D layer is shown in Figure 2d. The structural network of **2** can be represented as well-insulated layers of penta-coordinated Cu(II) cations in the unit cell.

**Crystal Structure of 3.** X-ray determination reveals that **3** is composed of isolated 1D azido-copper chains including the same *syn*−*syn* carboxylate and EO ($\mu$-1,1)-azido bridging modes existed in **1**. Unlike **1**, the solvent ethanol molecule is introduced as the third bridging ligands via $\mu$2 mode to coordinate with the adjacent Cu(II) cations, generating the triple bridging azido/carboxylate/ethanol Cu(II) chain in **3**. One crystallographic Cu(II) cation located at the inversion center forms the hexa-coordinated environment through an $N_2O_4$ group in which two azido N atoms and two carboxylate O atoms [Cu−N1 = 1.988 Å, Cu−O1 = 1.952 Å, Cu−N1A = 1.994 Å, and Cu−O2 = 1.935 Å] occupy the equatorial positions, while two oxygen atoms from two ethanol molecules locate in apical positions [Cu−O3 = 2.525 Å, Cu−O3A = 2.449 Å] (Figure 3a). Cu(II) cation presents a stretched octahedral geometry that was due to the typical Jahn−Teller distortion. Adjacent Cu(II) cations are linked by a carboxylate and an azido bridge, as well as an ethanol bridge, forming the 1D Cu(II) chain (Figure 3b). The coordination of ethanol shorten the intrachain separation between adjacent Cu ions [Cu1−Cu1A = 3.182 Å] than the Cu−Cu distance in **1**. As shown in Table S1 in the Supporting Information, the Cu1−N−Cu1A angle (106.0°) is in the normal range of EO bridging mode. The 1D chains are connected by interchain hydrogen-bonding between the ethanol molecule and azido anion [O3−H···N3A] (Figure S2 in the Supporting Information), which might transmit magnetic interactions. The closest distance of interchain Cu(II) cations is 7.682 Å.

**Thermogravimetric Analysis of 3.** According to the structural distinction of two types of 1D azido-Cu chians in compounds **1** and **3**, the thermal decomposition of compound **3** has been investigated with a small quantity of milligrams, because of the explosibility of azides. As shown in Figure S3 in the Supporting Information, **3** first undergoes a weight loss of 13.92% during the temperature interval from 93 °C to 140 °C, the weight loss corresponds to ethanol molecules (14.25%).


dx.doi.org/10.1021/ic5010769 | Inorg. Chem. 2014, 53, 8088−8097

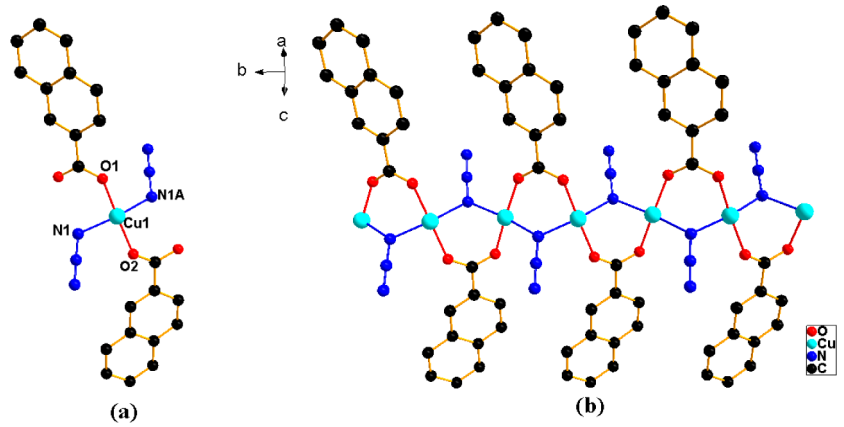


**Figure 1.** (a) Coordination environment of the Cu center in **1**. (b) Chain with mixed carboxylate and azido bridges for **1**. (Hydrogen atoms are omitted for the sake of clarity.)

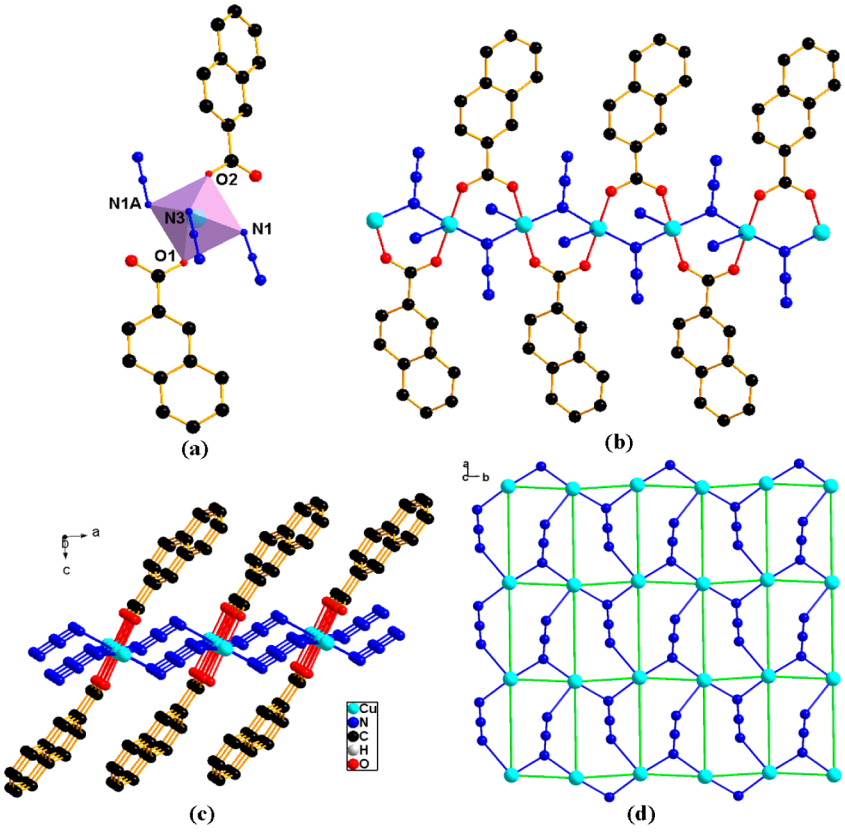


**Figure 2.** (a) Coordination environment of Cu center in **2**. (b) 1D chain with carboxylate and azido bridges for **2**. (c) 2D layer linked by EE-azido groups for **2**. (d) Simplified graphic of the 2D layer for **2**. (Hydrogen atoms are omitted for the sake of clarity.)

Furthermore, there is a continuous stable stage from 140 °C to 220 °C upon removing all ethanol molecules, which shows that the remainder structure probably remains consistent with the 1D azido-Cu chain existing in **1**. Following this observation, we continued to heat **3** at a constant temperature of 140 °C for half an hour and yielded the green homogeneous powders of dealcoholization product as compound **1b**. IR spectroscopy analysis reveals that, compared to **3**, the absence of the peaks at ~3418, 2974, and 1079 $cm^{-1}$ indicates that there are no coordinated ethanol molecules in **1b**. The measured PXRD patterns of **1b** and **1** closely matches that simulated from single-crystal diffraction data of **1**, indicating the azido-Cu chain structure maintenance upon ethanol removal (see Figure S4 in the Supporting Information). Turning back to the TG curve, it is seen that the intermediate displays a weight loss of 63.02% from 220 °C to 268 °C, which is due to the completely decomposition of compound **3**. The final residual mass is 23.06% of the initial mass, coincident with the calculation value of CuO (24.78%) determined by PXRD (Joint Committee for Powder Difraction Standards (JCPDS) File Card No. 05-0661).

**Magnetic Property.** Magnetic measurements have been performed on polycrystalline samples of compounds **1**−**3**, the phase purity of the bulk materials are confirmed by PXRD (Figure S4 in the Supporting Information). Based on the experimental results, the dominant ferromagnetic coupling between Cu(II) cations in compounds **1**−**3** can be proposed.


dx.doi.org/10.1021/ic5010769 | *Inorg. Chem.* 2014, 53, 8088−8097

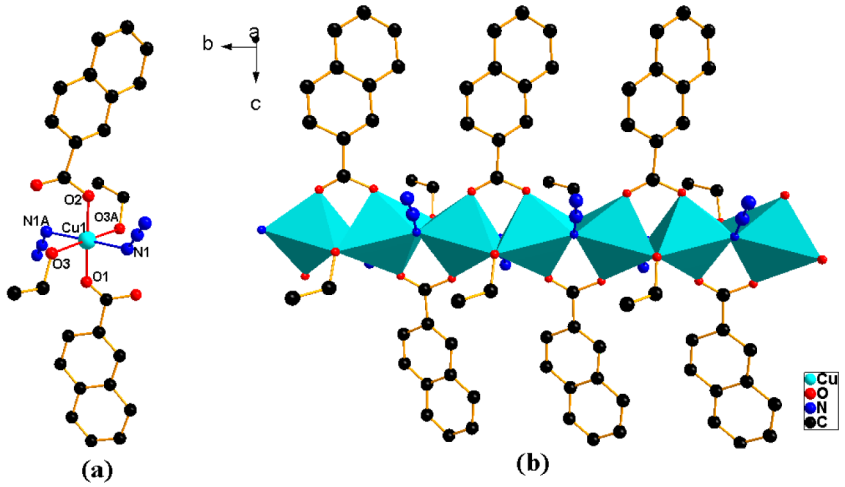


**Figure 3.** (a) Coordination environment of the Cu center in **3**. (b) The chain with mixed ethanol oxygen, carboxylate, and azido bridges for **3**. (Hydrogen atoms are omitted for clarity.)

However, in the low-temperature range, three compounds present distinguishing magnetic behaviors because of different structures, as discussed below.

**Magnetic Property of 1.** Magnetic susceptibility data of **1** is obtained in the range of 1.9−300 K (Figure 4). The room-temperature $\chi_M T$ value of **1** is ~0.56 cm$^3$ K mol$^{-1}$, which is higher than the spin-only value (0.375 cm$^3$ K mol$^{-1}$) for an magnetically isolated Cu(II) cation. Upon cooling, the $\chi_M T$ value increases to 4.48 cm$^3$ K mol$^{-1}$ at 5 K, suggesting ferromagnetic interaction between Cu(II) cations and finally drops to 1.67 cm$^3$ K mol$^{-1}$ at 1.9 K. The $\chi_M T$ vs $T$ curve illustrates that strongly coupled ferromagnetic system accompanies with AF interaction between the azido-Cu(II) chains in the compound **1**, noticeable only at low temperatures. The best-fit parameters through the Curie−Weiss law above 70 K are $C$ = 0.50 cm$^3$ K mol$^{-1}$ and $\Theta$ = 38.62 K, the $\Theta$ value supports strong ferromagnetic interaction in **1** (Figure 4). Using Baker's equation for the 1D chain of $S = {}^1/_2$ spins,[20] the experimental data can be simulated based on the Hamiltonian $\hat{H} = -J\sum\hat{S}_i\hat{S}_i$. As shown in Figure 4, the best fit obtains the following parameters: $g$ = 2.27, $J$ = 63.76 cm$^{-1}$, and $R = 6.72 \times 10^{-4}$ ($R = \sum[(\chi_M T)_{obsd} - (\chi_M T)_{calcd}]^2/\sum[(\chi_M T)_{obsd}]^2$). The large $J$ value demonstrates strong ferromagnetic coupling between the Cu(II) centers. It seems that AF coupling would be predicted for **1** due to the carboxylate group with *syn*−*syn* mode and the EO-azido with the Cu−N−Cu angle of 120.9°.[21]

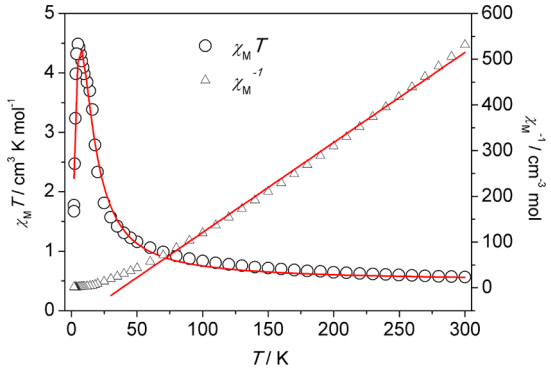


**Figure 4.** $\chi_M T$ vs $T$ and $1/\chi_m$ vs $T$ plots for **1**; the solid line is the fit to the experimental data and the fit to the Curie−Weiss law, respectively.

However, according to the proposition from Thompson et al. and Escuer et al., the countercomplementarity function derived from two types of ligands may expound the strong ferromagnetic interaction, not just the total of the two isolated components.[22] The field dependence on the magnetizations $M(H)$ is measured at 2 K and the fields up to 5 T for **1**. As shown in Figure 5, the curve rapidly reaches the saturation value (1.0 N$\beta$) for **1**, which is consistent with one Cu(II) cation at the higher fields. Notably, the S-shaped curve emerges with a critical field of 1500 Oe at low field (Figure 5, inset), indicating the interchain AF exchange and **1** is of a metamagnet. Magnetization hysteresis is another important characteristic of the magnetic bistability of magnet, so the dc magnetization is determined at 2.5, 4, and 6 K within ±7 kOe (see Figure S5 in the Supporting Information). When the temperature goes down to 2.5 K, a narrow-fissured hysteresis loop emerges with tiny coercive field and remnant magnetization (Figure S5 in the Supporting Information, inset). The ZFC/FC plots indicates the occurrence of spontaneous magnetization below 18 K for **1** (see Figure S6 in the Supporting Information), illustrating the appearance of the ferromagnetic state.

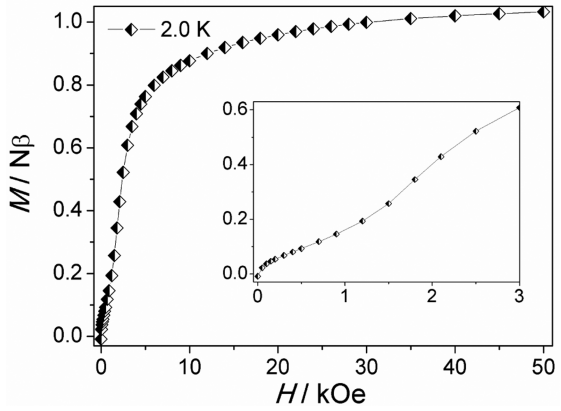


**Figure 5.** Magnetization vs $H$ plots for **1**. Inset shows the magnetization vs $H$ plots in the fields of 0−3 kOe.

Under the oscillating field of 3.5 Oe, the zero-field AC susceptibility experiments were determined in the range of 2−18 K and frequencies of 1, 3, 10, 33, 100, 333, and 1000 Hz, as


dx.doi.org/10.1021/ic5010769 | *Inorg. Chem.* 2014, 53, 8088−8097

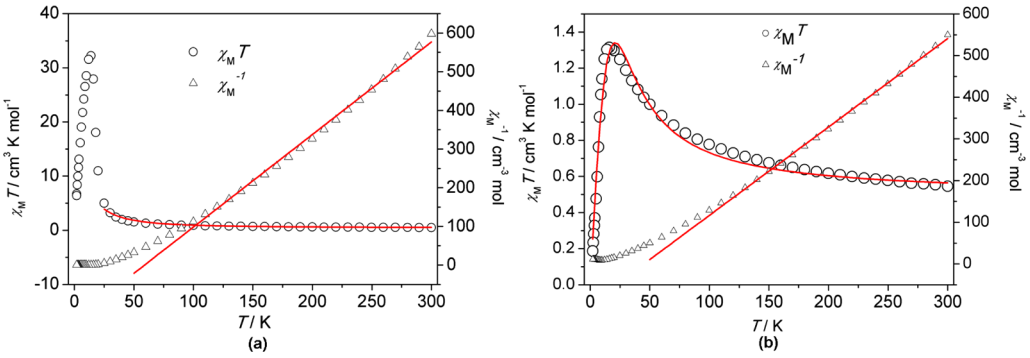


**Figure 6.** (a) $\chi_M T$ vs $T$ and $1/\chi_m$ vs $T$ plots for **2**. (b) $\chi_M T$ vs $T$ and $1/\chi_m$ vs $T$ plots for **3**. The solid line is the fit to the experimental data and the fit to the Curie–Weiss law, respectively.

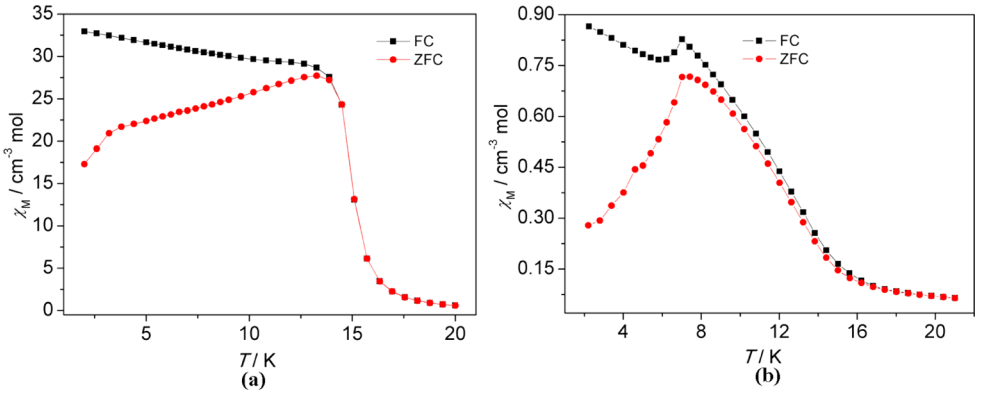


**Figure 7.** FC and ZFC plots for (a) **2** and (b) **3**.

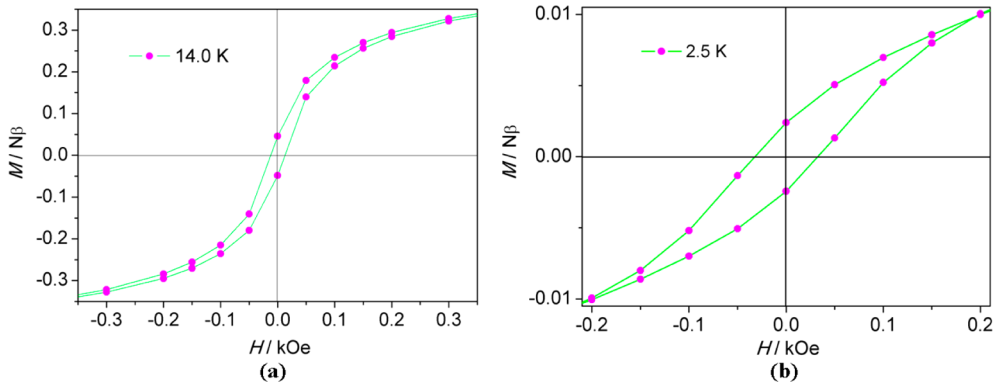


**Figure 8.** (a) Hysteresis loop of **2** at 14 K with an enlargement of the low-field region. (b) Hysteresis loop of **3** at 2.5 K with an enlargement of the low-field region.

shown in Figure S7 in the Supporting Information, exhibiting the occurrence of the magnetic ordering in **2**. A strong out-of-phase signal appears at 15 K, as the diminution of the in-phase signal arises, proving the performance of long-range ordering and slow magnetic relaxation in the system, but there is no out-of-phase peak until the temperature decreases to 2 K.

**Magnetic Properties of 2 and 3.** In the low-temperature range, the magnetism of **2** and **3** shows spontaneous magnetization. As shown in Figure 6, the $\chi_M T$ values are observed as 0.50 cm$^3$ K mol$^{-1}$ and 0.55 cm$^3$ K mol$^{-1}$for **2** and **3** at 300 K, respectively, larger than the spin-only value (0.375 cm$^3$ K mol$^{-1}$) for an isolated Cu(II) cation ($S = {}^1/_2$). As the temperature decreasing, the $\chi_M T$ values increase gradually, the pronounced rises are observed until below 30 K for **2** and 50 K for **3**, respectively. The maximal values arrive at 14 K for **2** and 16 K for **3**. As shown in Figure 6, the parameters fitted by the Curie–Weiss law above 100 K are obtained to be $C$ = 0.42 cm$^3$ K mol$^{-1}$ and $\Theta$ = 58.87 K for **2** and $C$ = 0.47 cm$^3$ K mol$^{-1}$ and $\Theta$ = 45.1 K for **3**. The positive $\Theta$ values suggest strong ferromagnetic interaction between the Cu(II) cations in **2** and **3**. The experimental data of **2** can be fitted based on the intrachain coupling $J$ ($\hat{H} = -J\sum\hat{S}_i\hat{S}_i$) together with the mean-field approximation[20] for interchain coupling $zJ'$. The best fit leads to $g$ = 2.01, $J$ = 135.08 cm$^{-1}$, $zJ'$ = −0.09 cm$^{-1}$, and $R$ = 1.38 × 10$^{-4}$ ($R = \sum[(\chi_M T)_{obsd} - (\chi_M T)_{calcd}]^2/\sum[(\chi_M T)_{obsd}]^2$) above 25 K (see Figure 6a). Considering the mean-field approximation,[23] the magnetic data of **3** was also simulated. The best fit leads to $g$ = 2.28, $J$ = 65.27 cm$^{-1}$, $zJ'$ = −2.06 cm$^{-1}$, and $R$ = 7.32 × 10$^{-4}$ ($R = \sum[(\chi_M T)_{obsd} - (\chi_M T)_{calcd}]^2/\sum[(\chi_M T)_{obsd}]^2$) (see Figure 6b). The $zJ'$ value is considered to


dx.doi.org/10.1021/ic5010769 | Inorg. Chem. 2014, 53, 8088–8097

be the interlayer and interchain interactions. However, the interlayer interactions are very weak because of the layers are well-separated. The field dependent on the magnetizations $M(H)$ at 2 K exhibits spontaneous magnetization to the saturation point of 0.98, which illustrates the existence of ferromagnetic order in **2** (see Figure S8a in the Supporting Information). For **3**, magnetization increases smoothly as the field rises and tends to saturation (1.04 N$\beta$) until 5 T at 2 K (see Figure S8b in the Supporting Information), which may be due to the antiferromagnetic-to-paramagnetic transition. A slightly twisted curve is observed at low field indicating the interchain AF coupling (Figure S8b in, inset the Supporting Information).

Moreover, the ZFC/FC curves for **2** and **3** display spontaneous magnetization below 20 K (Figure 7a) and 21 K (Figure 7b), respectively, illustrating the appearance of ferromagnetic state. The dc magnetizations of **2** and **3** are measured within ±7 kOe at different temperatures (see Figure S9 in the Supporting Information). A butterfly-shaped hysteresis loop emerges when the temperature are 14 K for **2** and 2.5 K for **3** (Figure 8), with the coercive fields of 10 and 31 Oe, and the remnant magnetizations of 0.047 N$\beta$ and 0.002 N$\beta$, respectively. Compounds **2** and **3** are considered as ordered magnets.

The experiment of the ac magnetic susceptibility was also carried out for **2**. The $\chi''_M$ vs $T$ plots at 15 K show a strong out-of-phase signal with weakly frequency dependent, showing slow dynamics of magnetization and occurrence of long-rang ferromagnetic ordering (Figure 9). The peak temperatures

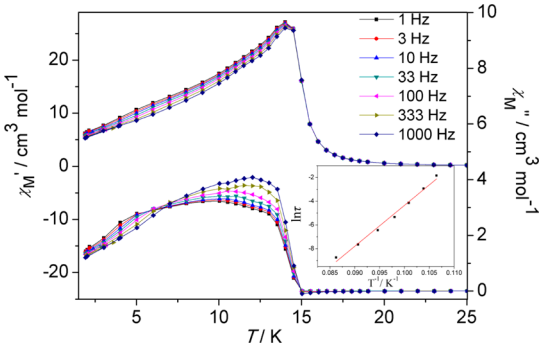


**Figure 9.** $\chi'_M$ and $\chi''_M$ vs $T$ vs plots for **2**.

($T_p$) in $\chi''_M$ shift from 9.23 to 11.61 K with frequency increasing from 1 Hz to 1000 Hz. The parameter $\Phi = (\Delta T_p/T_p)/\Delta(\log f) = 0.09$ reveals the slow magnetic relaxation and deviates from the typical range ($0.1 \leq \Phi \leq 0.3$) of the superparamagnetic materials.[24] Plotting ln $\tau$ against $1/T$ has been fitted following the Arrhenius equation $\tau = \tau_0 \exp(\Delta E/k_B T)$ ($\tau$ is the relaxation time) (Figure 9, inset). The calculated $\tau_0$ ($1.4 \times 10^{-17}$ s) clearly indicates that **2** shows the typical spin glass (SG) behavior[25] rather than superparamagnetic behavior ($10^{-6}$ to $10^{-13}$s).[1c] The AC magnetic susceptibility plots of **3** indicates a strong out-of-phase $\chi''_M$ signal at 12 K lower than that of **2** (Figure 10). The maximum positions of out-of-phase signal are dependent on frequency slightly, determining the existence of slow magnetic relaxation. The peak temperatures ($T_p$) of the out-of-phase curve moves from 6.96 to 7.35 K as the frequency shifts from 1 to 1000 Hz. The $\Phi$ value is obtained as 0.02, which is consistent with the values of spin glass ($\Phi \leq 0.08$)[25] and indicates a weakly slow magnetic

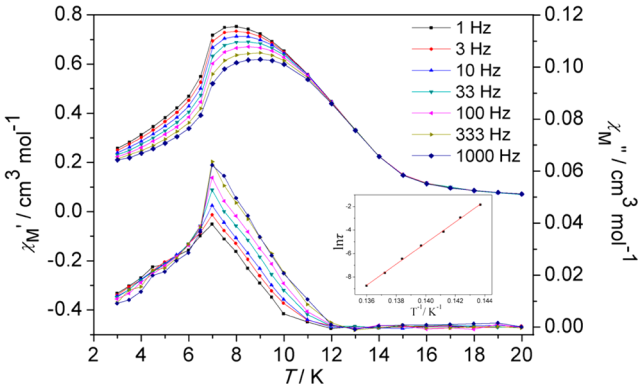


**Figure 10.** $\chi'_M$ and $\chi''_M$ $T$ plots for **3**.

relaxation. The frequency dependence of $T_p$ on the out-of-phase signal has also been modeled by the Arrhenius equation (Figure 10, inset), like **2**, the rather small value of $\tau_0$ ($1.7 \times 10^{-57}$ s) obviously indicates the characteristic of SG phase as well.[25]

**Thermodynamics of 1 and 2 with DFT.** To better understand the formations of two isomeric compounds on the base of essential principle in chemical thermodynamics, we have employed the DFT approach to explore the thermodynamic stability of compounds **1** and **2**. To begin with, the calculations of structural optimization were performed using Generalized Gradient Approximation (GGA- PBE) method with CASTEP software package.[26] The stable state energies of **1** and **2** were calculated as −730.8530768 and −730.8597720 hartree, respectively, the difference values of 0.0066952 hartree (17.6 kJ mol$^{-1}$) between two compounds is shown in Figure 11. Thermodynamically, it is obvious that compound **2** stands

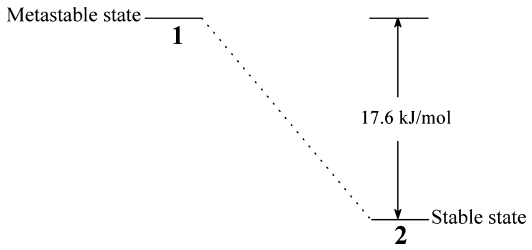


**Figure 11.** Stable state energies for **1** and **2**.

in the stable state and **1** can be considered as the thermodynamical metastable state, which corresponding the different solvent systems during the synthetic process.

**Discussion.** Two isomeric Cu(II) compounds—**1** and **2**—are synthesized with azido and 2-Hna ligands in different solvents, probably due to different vapor pressures in the hydro(solvo)thermal treatment (429.92 kPa for ethanol solution and 198.48 kPa for aqueous solution at 120 °C), as well as **2** either could be obtained from **1** in the aqueous solution at 120 °C. As the product of higher pressure, **1** is identified as thermodynamical metastable state with 1D carboxylate/EO-azido copper chain, while **2** is stable state with 2D layer-like structure extended by EE-azido bridging. The interesting structural feature of two compounds is that the 2D layer in **2** is a combination of the 1D chain in **1**. Notably, compound **3** is yielded by the SCSC transformation from **1** in the ethanol solution in which the oxygen atoms connect to Cu(II) cations forming a triple bridging azido/carboxylate/


dx.doi.org/10.1021/ic5010769 | Inorg. Chem. 2014, 53, 8088−8097

ethanol Cu(II) chain in **3**. Interestingly, **3** could be restored to **1** with powder state (**1b**) through dealcoholization under heating condition. The fascinating point is that the three compounds cover three types of coordination geometries of Cu(II) cations, respectively. And then, different structures lead to different magnetic behaviors.

In **1**, the possible pathways of magnetic transmission along the copper chains are provided by the EO-azido and *syn,syn*-carboxylate ligands. The critical parameters Cu−N distance and Cu−N−Cu angle are of 1.97 Å and 120.9°, as well as the intrachain and interchain Cu−Cu distances are of 3.433 and 8.155 Å, respectively (see Figure 12a). As studied by Ruiz et al.

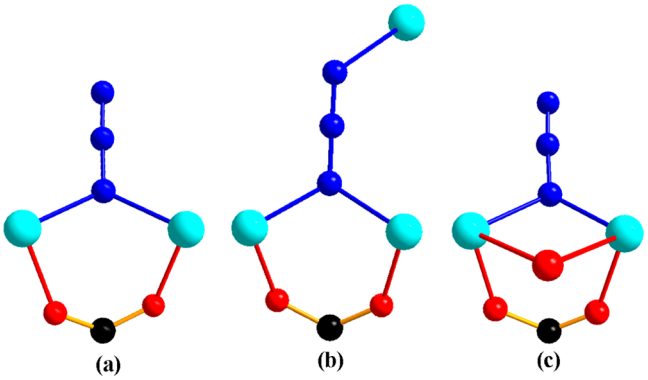


**Figure 12.** Magnetic exchanges of Cu(II) cations in compounds: (a) for **1**, (b) for **2**, (c) for **3**.

for planar $[Cu_2(EO{-}N_3)_2]$ units,[27] the EO−azide groups showing large Cu−N−Cu angles in **1** should offer AF exchange. However, the ferromagnetic coupling exists in **1**. The magnetic orbit of the Cu(II) cation is tilted $d_{x^2-y^2}$ (Figure 7a), generating the nonplanar $[Cu_2(EO\text{-}N_3)_2]$ units. Furthermore, the *syn,syn*-carboxylato group may lead to the countercomplementarity effect, not just the total of the two isolated interactions. All of these result in ferromagnetic exchange.[28]

For **2**, two types of magnetic exchange pathways can be described in two directions of the 2D layers (Figure 12b): (a) As done for **1**, the magnetic transmission along the copper chains are provided by the EO−azido and *syn,syn*-carboxylate ligands. The critical parameters Cu−N distance and Cu−N−Cu angle are of 1.98−2.00 Å and 111.7°, as well as the intrachain and interchain Cu−Cu distances are of 3.295 and 5.06 Å, respectively. (b) In the vertical direction, the EE−azido ligands link all 1D chains to form the 2D layer, which provides a weakly AF coupling pathway by bridging full $d_{z^2}$ orbits to the half-full $d_{x^2-y^2}$ orbits of the Cu(II) cations in the adjacent chains. The $\mu$-1,1,3-N3 only connect to one Cu(II) cation leading to half EE−azido magnetic coupling pathways since the Cu(II) cations exhibit penta-coordinated geometry in **2** (Figure 7b), which is likely attributed to the steric hindrance of the naphthalene ring and is the most probably reason for slight influence on the appearance of ferromagnetic state at low-temperature range. In summary, compound **2** presents spin glass behavior.

There exist three types of intrachain magnetic exchange paths in **3** (Figure 12c). Compared with **1**, the similar paths are afforded by *syn,syn*-carboxylate and EO-azido ligands (Cu−N = 1.99 Å, Cu−N−Cu = 106.0°), and the added path is that the ethanol molecules connect to hexa-coordinated Cu(II) cations at axial location (Cu−O = 2.45−2.53 Å). Meanwhile, the intrachain and interchain Cu−Cu distances are determined to be 3.182 and 7.682 Å, respectively. Obviously, the bridging of solvent oxygen atom shortens the distance of intrachain Cu(II) cations than that of **1**. Just like **1**, the counter complementarity effect derived from three types of ligands may explicate the existence of ferromagnetic interaction. Finally, the glasslike behavior is observed in **3** as well.

As we notice, the difference of intrachain $J$ values in compounds **1**−**3** responds to the different parameters of the Cu−Cu distance and Cu−N−Cu angle. This is coincident with the previously reported Cu(II) compounds with EO-azido/carboxylato ligands. Obviously, the ferromagnetic exchange in the azido-Cu(II) compounds improves with the decreases of the Cu−Cu distance and Cu−N−Cu angle, with the relatively larger $J$ values near the range of Cu−Cu distance with 3.2−3.3 Å and Cu−N−Cu angle with 107°−112°. The related information is listed in Table 2. All of the coupling constants $J$ are in accord with two Cu(II) cations linked by EO−azido and carboxylate groups, which are afforded by the Hamiltonian $\hat{H} = -J\sum\hat{S}_i\hat{S}_i$.

**Table 2. Related Cu−Cu Distances, Cu−N−Cu Angles, and Coupling Constants for the Carboxylato/EO Azido Mixed-Bridged Copper Compounds**

| Cu−Cu distance (Å) | Cu−N−Cu angle (deg) | $J$ (cm$^{-1}$) | ref |
|---|---|---|---|
| 3.537 | 126.8 | 39 | ref 7b |
| 3.522 | 124.3 | 48 | ref 7d |
| 3.433 | 120.9 | 67.8 | **1** (this work) |
| 3.409 | 116.9 | 69.7 | ref 7b |
| 3.386 | 116.1 | 69.7 | ref 7e |
| 3.284 | 111.9 | 75 | ref 4b |
| 3.295 | 111.7 | 135.1 | **2** (this work) |
| 3.230 | 108.2 | 93.10 | ref 7b |
| 3.219 | 107.6 | 126 | ref 4c |
| 3.200 | 106.7 | 80 ± 5 | ref 4d |
| 3.216 | 106.6 | 80 | ref 7b |
| 3.190 | 106.5 | 126 | ref 4c |
| 3.182 | 106.0 | 65.3 | **3** (this work) |
| 3.185 | 105.5 | 63 | ref 4e |
| 3.120 | 103.0 | 89 | ref 7d |

## CONCLUSIONS

Three azido-Cu(II) compounds with 2-naphthoic acid (2-na) as a co-ligand have been successfully obtained in different solvent systems, as well as structurally and magnetically characterized. The Cu(II) cations exhibit tetra-, penta-, and hexa-coordination geometries in compounds **1**−**3**, respectively. For isomeric **1** and **2**, although having the same chemical formula, $[Cu(2\text{-na})(N_3)]$, display different structures of well-isolated 1D chain with $\mu$-1,1-azido and 2D layer with $\mu$-1,1,3-azido, respectively. DFT calculation reveals that **2** features superior thermodynamic stability than **1**. Compound **3** composed of a triple bridging 1D chain with $\mu$-1,1-azido is derived from **1** through SCSC transformation, when the heating−dealcoholization of **3** reversely leads to **1**. Different structures result in different magnetisms in three compounds. Spontaneous magnetizations occur in compounds **1**−**3** with transition temperatures of 15, 15, and 12 K. In summary, compound **1** is of a metamagnet, while compounds **2** and **3** represent spin glass behavior.


dx.doi.org/10.1021/ic5010769 | *Inorg. Chem.* 2014, 53, 8088−8097

## ■ ASSOCIATED CONTENT

### Supporting Information

Table S1 and Figures S1−S9, crystal structures of compounds **1**−**3** in CIF format. CCDC numbers for **1**−**3** (Nos. 992772, 992773, and 992774, respectively). These data can be obtained free of charge from the Cambridge Crystallographic Data Centre via www.ccdc.cam.ac.uk/data_request/cif. This material is available free of charge via the Internet at http://pubs.acs.org.

## ■ AUTHOR INFORMATION

### Corresponding Author

*Tel.: +86-029-88302604. Fax: +86-029-88302604. E-mail: sanpingchen@126.com.

### Notes

The authors declare no competing financial interest.

## ■ ACKNOWLEDGMENTS

The present research was supported by the National Natural Science Foundation of China (Nos. 21073142, 21173168, and 21373162), and the Nature Science Foundation of Shanxi Province (Nos. SJ08B09, FF10091, and 11JS110).

## ■ REFERENCES

(1) (a) Ferlay, S.; Mallah, T.; Ouahes, R.; Veillet, P.; Verdaguer, M. *Nature* **1995**, *378*, 701−703. (b) Entley, W. R.; Girolami, G. S. *Science* **1995**, *268*, 397−397. (c) Sun, H.-L.; Wang, Z.-M.; Gao, S. *Coord. Chem. Rev.* **2010**, *254*, 1081−1100. (d) Campbell, V. E.; Guillot, R.; Riviere, E.; Brun, P. T.; Wernsdorfer, W.; Mallah, T. *Inorg. Chem.* **2013**, *52*, 5194−5200. (e) Zheng, Y.-Z.; Zheng, Z.; Chen, X.-M. *Coord. Chem. Rev.* **2014**, *258*, 1−15. (f) Pardo, E.; Faus, J.; Julve, M.; Lloret, F.; Muñoz, M. C.; Cano, J.; Ruiz-García, R. *J. Am. Chem. Soc.* **2003**, *125*, 10770−10771.

(2) (a) Ritter, S. K. *Chem. Eng. News.* **2004**, *82*, 29−32. (b) Gatteschi, D.; Sessoli, R. *Angew. Chem., Int. Ed.* **2003**, *42*, 268−297. (c) Wernsdorfer, W.; Aliaga-Alcalde, N.; Hendrickson, D. N.; Christou, G. *Nature* **2002**, *416*, 406−409. (d) Woodruff, D. N.; Winpenny, R. E.; Layfield, R. A. *Chem. Rew.* **2013**, *113*, 5110−5148. (e) Leng, J.-D.; Liu, J.-L.; Zheng, Y.-Z.; Ungur, L.; Chibotaru, L. F.; Guo, F.-S.; Tong, M.-L. *Chem. Commun.* **2013**, *49*, 158−160.

(3) (a) Caneschi, A.; Gatteschi, D.; Lalioti, N.; Sangregorio, C.; Sessoli, R.; Venturi, G.; Vindigni, A.; Rettori, A.; Pini, M. G.; Novak, M. A. *Angew. Chem., Int. Ed.* **2001**, *40*, 1760−1763. (b) Tangoulis, V.; Lalia-Kantouri, M.; Gdaniec, M.; Papadopoulos, C.; Miletic, V.; Czapik. *Inorg. Chem.* **2013**, *52*, 6559−6569. (c) Lescouëzec, R.; Vaissermann, J.; Ruiz-Pérez, C.; Lloret, F.; Carrasco, R.; Julve, M.; Verdaguer, M.; Dromzee, Y.; Gatteschi, D.; Wernsdorfer, W. *Angew. Chem., Int. Ed.* **2003**, *42*, 1483−1486. (d) Wang, Y.-Q.; Cheng, A.-L.; Liu, P.-P.; Gao, E.-Q. *Chem. Commun.* **2013**, *49*, 6995−6997. (e) Pardo, E.; Ruiz-García, R.; Lloret, F.; Faus, J.; Julve, M.; Journaux, Y.; Ruiz-Pérez, C. *Chem.—Eur. J.* **2007**, *13*, 2054−2066.

(4) (a) Pereira, C. L. M.; Pedroso, E. F.; Stumpf, H. O.; Novak, M. A.; Ricard, L.; Ruiz-Garcıa, R.; Riviere, E.; Journaux, Y. *Angew. Chem., Int. Ed.* **2004**, *43*, 956−958. (b) Tangoulis, V.; Panagoulis, D.; Raptopoulou, C. P.; Samara, C. D. *Dalton Trans.* **2008**, 1752−1760. (c) Zeng, Y.-F.; Liu, F.-C.; Zhao, J.-P.; Cai, S.; Bu, X.-H.; Ribas, J. *Chem. Commun.* **2006**, 2227−2229. (d) Han, Y.-F.; Wang, T.-W.; Song, Y.; Shen, Z.; You, X.-Z. *Inorg. Chem.* **2008**, *11*, 207−210. (e) Zou, J.-Y.; Shi, W.; Gao, H.-L.; Cui, J.-Z.; Cheng, P. *Inorg. Chem. Front.* **2014**, *1*, 242−248.

(5) (a) Ribas, J.; Escuer, A.; Monfort, M.; Vicente, R.; Cortes, R.; Lezama, L.; Rojo, T. *Coord. Chem. Rev.* **1999**, *193*, 1027−1068. (b) Kurmoo, M. *Chem. Soc. Rev.* **2009**, *38*, 1353−1379. (c) Zeng, Y.-F.; Hu, X.; Liu, F.-C.; Bu, X.-H. *Chem. Soc. Rev.* **2009**, *38*, 469−480. (d) Banerjee, S.; Adhikary, C.; Rizzoli, C.; Pal, R. *Inorg. Chim. Acta* **2014**, *409*, 202−207. (e) Bhargavi, G.; Rajasekharan, M. V.; Costes, J. P.; Tuchagues, J. P. *Dalton Trans.* **2013**, *42*, 8113−8123.

(6) (a) *Magnetism: Molecules to Materials*; Miller, J. S., Drillon, M., Eds.; Wiley−VCH: Weinheim, Germany, 2002. (b) Kahn, O. *Molecular Magnetism*; VCH: New York, 1993. (c) Liu, J.; Qin, Y. L.; Qu, M.; Clérac, R.; Zhang, X. M. *Dalton Trans.* **2013**, *42*, 11571−11575.

(7) (a) Abu-Youssef, M. A. M.; Escuer, A.; Gatteschi, D.; Goher, M. A. S.; Mautner, F. A.; Vicente, R. *Inorg. Chem.* **1999**, *38*, 5716−5723. (b) Zhao, J.-P.; Hu, B.-W.; Sañudo, E. C.; Yang, Q.; Zeng, Y.-F.; Bu, X.-H. *Inorg. Chem.* **2009**, *48*, 2482−2489. (c) Mukherjee, P. S.; Dalai, S.; Zangrando, E.; Lloretc, F.; Chaudhuri, N. R. *Chem. Commun.* **2001**, 1444−1445. (d) He, Z.; Wang, Z.-M.; Gao, S.; Yan, C.-H. *Inorg. Chem.* **2006**, *45*, 6694−6705. (e) Tommasino, J. B.; Chastanet, G.; Le Guennic, B.; Robert, V.; Pilet, G. *New J. Chem.* **2012**, *36*, 2228−2235. (f) Yang, L.; Zhang, S.; Liu, X.; Yang, Q.; Wei, Q.; Xie, G.; Chen, S. *CrystEngComm.* **2014**, *16*, 4194−4201.

(8) (a) Escuer, A.; Cano, J.; Goher, M. A. S.; Journaux, Y.; Lloret, F.; Mautner, F. A.; Vicente, R. *Inorg. Chem.* **2000**, *39*, 4688−4695. (b) Escuer, A.; Mautner, F. A.; Goher, M. A. S.; Abu-Youssef, M. A. M.; Vicente, R. *Chem. Commun.* **2005**, 605−607. (c) Gao, E.-Q.; Yue, Y.-F.; Bai, S.-Q.; He, Z.; Zhang, S.-W.; Yan, C.-H. *Chem. Mater.* **2004**, *16*, 1590−1596. (d) Chakraborty, A.; Rao, L. S.; Manna, A. K.; Pati, S. K.; Ribas, J.; Maji, T. K. *Dalton. Trans.* **2013**, *42*, 10707−10714. (e) Zhang, Q.; Zhang, H.; Zeng, S.; Sun, D.; Zhang, C. *Asian J. Chem.* **2013**, *8*, 1985−1989.

(9) (a) Zeng, Y.-F.; Hu, X.; Liu, F.-C.; Bu, X.-H. *Chem. Soc. Rev.* **2009**, *38*, 469−480. (b) Maji, T. K.; Mukherjee, P. S.; Mostafa, G.; Mallah, T.; Cano-Boquera, J.; Chaudhuri, N. R. *Chem. Commun.* **2001**, 1012−1013. (c) Liu, T.-F.; Fu, D.; Gao, S.; Zhang, Y.-Z.; Sun, H.-L.; Su, G.; Liu, Y.-J. *J. Am. Chem. Soc.* **2003**, *125*, 13976−13977. (d) Zhao, J.-P.; Zhao, R.; Song, W.-C.; Yang, Q.; Liu, F.-C.; Bu, X.-H. *Cryst. Growth. Des.* **2013**, *13*, 437−439. (e) Yoo, H. S.; Kim, J. I.; Yang, N.; Koh, E. K.; Park, J. G.; Hong, C. S. *Inorg. Chem.* **2007**, *46*, 9054−9056. (f) Yang, Q.; Zhang, X.-F.; Zhao, J.-P.; Hu, B.-W.; Bu, X.-H. *Cryst. Growth. Des.* **2011**, *11*, 2839−2845. (g) Abu-Youssef, M. A. M.; Escuer, A.; Langer, V. *Eur. J. Inorg. Chem.* **2006**, *45*, 3177−3184.

(10) (a) Cortes, R.; Urtiaga, M. K.; Lezama, L.; Larramendi, J. I. R.; Arriortua, M. I.; Rojo, T. J. *Chem. Soc., Dalton Trans.* **1993**, 3685−3694. (b) Thompson, L. K.; Tandon, S. S. *Comments Inorg. Chem.* **1996**, *18*, 125−144. (c) Cabrero, J.; de Graaf, C.; Bordas, E.; Caballol, R.; Malrieu, J.-P. *Chem.—Eur. J.* **2003**, *9*, 2307−2315. (d) Triki, S.; García, C. J. G.; Ruiz, E.; Pala, J. S. *Inorg. Chem.* **2005**, *44*, 5501−5508. (e) Mialane, P.; Dolbecq, A.; Marrot, J.; Riviere, E.; Secheresse, F. *Chem.—Eur. J.* **2005**, *11*, 1771−1778.

(11) (a) Manson, J. L.; Arif, A. M.; Miller, J. S. *Chem. Commun.* **1999**, 1479−1480. (b) Fu, A.-H.; Huang, X.-Y.; Li, J.; Yuen, T.; Lin, C. L. *Chem.—Eur. J.* **2002**, *8*, 2239−2247. (c) Pramanik, K.; Malpaharia, P.; Mota, A. J.; Colacio, E.; Das, B.; Lloret, F.; Chandra, S. K. *Inorg. Chem.* **2013**, *52*, 3995−4001. (d) Tommasino, J. B.; Chastanet, G.; Guennic, B. L.; Robert, V.; Pilet, G. *New. J. Chem.* **2012**, *36*, 2228−2235.

(12) (a) Zheng, Y.-Z.; Tong, M.-L.; Zhang, W.-X.; Chen, X.-M. *Angew. Chem., Int. Ed.* **2006**, *45*, 6310−6314. (b) Bai, Y.-L.; Tao, J.; Wernsdorfer, W.; Sato, O.; Huang, R.-B.; Zheng, L.-S. *J. Am. Chem. Soc.* **2006**, *128*, 16428−16429. (c) Liu, F.-C.; Zeng, Y.-F.; Li, J.-R.; Bu, X.-H.; Zhang, H.-J.; Ribas, J. *Inorg. Chem.* **2005**, *44*, 7298−7300. (d) Zhang, X.-M.; Wang, Y.-Q.; Li, X.-B.; Gao, E.-Q. *Dalton Trans.* **2012**, *41*, 2026−2033. (e) Mukherjee, S.; Patil, Y. P.; Mukherjee, P. S. *Dalton Trans.* **2012**, *41*, 54−64.

(13) (a) Zhang, J.; Wojtas, L.; Larsen, R. W.; Eddaoudi, M.; Zaworotko, M. *J. Am. Chem. Soc.* **2009**, *131*, 17040−17041. (b) Li, C.-P.; Yu, Q.; Chen, J.; Du, M. *Cryst. Growth Des.* **2010**, *10*, 2650−2660. (c) Luo, L.; Chen, K.; Liu, Q.; Lu, Y.; Okamura, T.-a.; Lv, G.-C.; Zhao, Y.; Sun, W.-Y. *Cryst. Growth Des.* **2013**, *13*, 2312−2321. (d) Sun, D.; Ke, Y.; Collins, D. J.; Lorigan, G. A.; Zhou, H.-C. *Inorg. Chem.* **2007**, *46*, 2725−2734.

(14) (a) Xiao, J.; Liu, B. Y.; Wei, G.; Huang, X. C. *Inorg. Chem.* **2011**, *50*, 11032−11038. (b) Bajpai, A.; Venugopalan, P.; Moorthy, J. N. *Cryst. Growth Des.* **2013**, *13*, 4721−4729. (c) Dietzel, P. D.; Morita, Y.; Blom, R.; Fjellvåg, H. *Angew. Chem., Int. Ed.* **2005**, *117*, 6512−6516. (d) Zhang, X. M.; Hao, Z. M.; Zhang, W. X.; Chen, X. M. *Angew.*

*Chem., Int. Ed.* **2007**, *119*, 3526−3529. (e) Wriedt, M.; Yakovenko, A. A.; Halder, G. J.; Prosvirin, A. V.; Dunbar, K. R.; Zhou, H. C. *J. Am. Chem. Soc.* **2013**, *135*, 4040−4050.
(15) (a) Toh, N. L.; Nagarathinam, M.; Vittal, J. J. *Angew. Chem., Int. Ed.* **2005**, *44*, 2237−2241. (b) Kepert, C. J. *Chem. Commun.* **2006**, 695−700. (c) Kitagawa, S.; Kitaura, R.; Noro, S.-i. *Angew. Chem., Int. Ed.* **2004**, *43*, 2334−2375. (d) Zhang, B.; Wang, Z.-M.; Kurmoo, M.; Gao, S.; Inoue, K.; Kobayashi, H. *Adv. Funct. Mater.* **2007**, *17*, 577−584. (e) Xu, G.; Guo, G. C.; Wang, M. S.; Zhang, Z. J.; Chen, W. T.; Huang, J. S. *Angew. Chem., Int. Ed.* **2007**, *46*, 3249−3251. (f) Jhang, P. C.; Chuang, N. T.; Wang, S. L. *Angew. Chem., Int. Ed.* **2010**, *49*, 4200−4204. (g) Liu, D.; Ren, Z. G.; Li, H. X.; Lang, J. P.; Li, N. Y.; Abrahams, B. F. *Angew. Chem., Int. Ed.* **2010**, *49*, 4767−4770. (h) Avendano, C.; Zhang, Z.; Ota, A.; Zhao, H.; Dunbar, K. R. *Angew. Chem., Int. Ed.* **2011**, *50*, 6543−6547.
(16) (a) Kawano, M.; Fujita, M. *Coord. Chem. Rev.* **2007**, *251*, 2592−2606. (b) Liu, D.; Lang, J.; Abrahams, B. *J. Am. Chem. Soc.* **2011**, *133*, 11042−11045. (c) Reger, D. L.; Debreczeni, A.; Smith, M. D. *Inorg. Chem.* **2011**, *50*, 11754−11764. (d) Chen, M.-S.; Chen, M.; Takamizawa, S.; Okamura, T.-A.; Fan, J.; Sun, W.-Y. *Chem. Commun.* **2011**, *47*, 3787−3789. (e) Su, Z.; Chen, M.; Okamura, T.-A.; Chen, M. S.; Chen, S.-S.; Sun, W.-Y. *Inorg. Chem.* **2011**, *50*, 985−991. (f) Inokuma, Y.; Arai, T.; Fujita, M. *Nat. Chem.* **2010**, *2*, 780−783.
(17) (a) Tanabe, K. K.; Cohen, S. M. *Chem. Soc. Rev.* **2011**, *40*, 498−519. (b) Park, H. J.; Cheon, Y. E.; Suh, M. P. *Chem.—Eur. J.* **2010**, *16*, 11662−11669. (c) Reger, D. L.; Horger, J. J.; Smith, M. D. *Chem. Commun.* **2011**, *47*, 2805−2807.
(18) (a) Sheldrick, G. M. *SADABS, Program for Empirical Absorption Correction*; University of Göttingen, Göttingen, Germany, 1996. (b) Sheldrick, G. M.*SHELXTL*; Bruker Analytical X-ray Instruments, Inc.: Madison, WI, 1998.
(19) (a) Li, L.-C.; Jiang, Z.-H.; Liao, D.-Z.; Yan, S.-P.; Wang, G.-L. *Transition Met. Chem.* **2000**, *25*, 630−634. (b) Manikandan, P.; Muthukumaran, R.; Thomas, K. J.; Varghese, B.; Chandramouli, G.; Manoharan, P. *Inorg. Chem.* **2001**, *40*, 2378−2389. (c) Matsumoto, K.; Ooi, S. i.; Nakatsuka, K.; Mori, W.; Suzuki, S.; Nakahara, A.; Nakao, Y. *Dalton Trans.* **1985**, 2095−2100. (d) Cortés, R.; Urtiaga, M. K.; Lezama, L.; Larramendi, J. I. R.; Arriortua, M. I.; Rojo, T. *Dalton Trans.* **1993**, 3685−3694.
(20) Baker, G. A.; Rushbrooke, G. S. *Phys. Rev.* **1964**, *135*, 1272−1277.
(21) (a) Zeng, Y.-F.; Zhao, J.-P.; Hu, B.-W.; Hu, X.; Liu, F.-C.; Ribas, J.; Ribas-Ariño, J.; Bu, X.-H. *Chem.—Eur. J.* **2007**, *13*, 9924−9930. (b) Tangoulis, V.; Panagoulis, D.; Raptopoulou, C.; Dendrinou-Samara, C. *Dalton. Trans.* **2008**, 1752−1760. (c) Tandon, S. S.; Thompson, L. K.; Manuel, M. E.; Bridson, J. N. *Inorg. Chem.* **1994**, *33*, 5555−5570. (d) Thompson, L. K.; Tandon, S. S.; Manuel, M. E. *Inorg. Chem.* **1995**, *34*, 2356−2366.
(22) (a) Thompson, L. K.; Tandon, S. S.; Lloret, F.; Cano, J.; Julve, M. *Inorg. Chem.* **1997**, *36*, 3301−3306. (b) Escuer, A.; Vicente, R.; Mautner, F. A.; Goher, M. A. *Inorg. Chem.* **1997**, *36*, 1233−1236.
(23) (a) Myers, B. E.; Berger, L.; Friedberg, S. A. *J. Appl. Phys.* **1969**, *40*, 1149−1151. (b) O'Conner, C. J. *Prog. Inorg. Chem.* **1982**, *29*, 203−283.
(24) (a) Binder, K.; Young, A. P. *Rev. Mod. Phys.* **1986**, *58*, 801−976. (b) Rebilly, J.-N.; Mallah, T. *Struct. Bonding (Berlin)* **2006**, *122*, 103−131.
(25) Mydosh, J. A. *Spin Glasses: An Experimental Introduction*; Taylor & Francis: London, 1993.
(26) Segall, M.; Lindan, P.; Probert, M.; Pickard, C.; Hasnip, P.; Clark, S.; Payne, M. *J. Phys.: Condens. Matter* **2002**, *14*, 2717−2744.
(27) Ruiz, E.; Cano, J.; Alvarez, S.; Alemany, P. *J. Am. Chem. Soc.* **1998**, *120*, 11122−11129.
(28) Colacio, E.; Costes, J.-P.; Domínguez-Vera, J. M.; Maimounac, I. B.; Suárez-Varela, J. *Chem. Commun.* **2005**, 534−536.